Journal of Mathematics and Informatics
Vol. 29, 2025, 47-64
ISSN: 2349-0632 (P), 2349-0640 (online)
Published 30 December 2025
www.researchmathsci.org
DOI:http://doi.org/10.22457/jmi.v29a06266

Journal of
Mathematics and
Informatics

Hall Current Effects on Unsteady Magneto-Hydrodynamics Micropolar Fluid Flow in A Periodic Field Through an Infinite Vertical Plate

Md. Rafiqul Islam[1], Md. Aslam Hossain[1*] and Shaikh Khurram Alam[2]

[1]Department of Mathematics, Pabna University of Science and Technology, Pabna-6600, Bangladesh
[2]Mathematics Discipline, Khulna University, Khulna-9208, Bangladesh
[*]Corresponding author's email: aslam.math@pust.ac.bd

Received 31 October 2025; accepted 20 December 2025

Abstract. Micropolar fluids (MPF) can be useful in a variety of engineering purposes when traditional Newtonian fluid concepts are unable to represent the necessary behavior [18]. The possible uses of MPF flow in magnetic fields, including the creation of novel energy-producing and health-care innovations, are being eagerly investigated by investigators [16]. Based on the non-similarity studies, the consequences of Hall current on the movement of magneto-hydrodynamics (MHD) MPF flow across a sliding vertical plate has been investigated in this study. A flow model to express time-dependent momentum, rotational momentum, and energy equations is developed using a boundary-layer approximation. The explicit finite difference method (EFDM) based Compaq Visual Fortran 6.6a computational tool is employed to solve the governing equations. The accuracy of the numerical technique was checked using a stability and convergence analysis. The results showed that the system converged at the Prandtl number, $P_r \geq 0.25$, when $\tau = 0.005, \Delta X = 0.8$ and $\Delta Y = 0.2$ and that the spin gradient viscosity (λ) and vortex viscosity (Λ) depended on distinct values. The study's conclusions have been graphically represented for a range of known parameter values at different time points.

Keywords: MHD Periodic Field, Micropolar fluid, Hall Current, Explicit Finite Difference Method

AMS Mathematics Subject Classification (2020): 76E25

1. Introduction

The field of magneto fluid dynamics known as MHD studies the motion of electrically conducting fluids in both magnetic and electric fields. The study of astrophysics has perhaps contributed the most to our knowledge of such occurrences. It has long been believed that plasma or highly charged gases make up the great majority of the universe's matter. These experiments have contributed to the development of a large part of the fundamental understanding of electromagnetic fluid dynamics. Within the discipline of plasma physics, MHD examines the effects of electromagnetic fields on a continuous, electrically conducting fluid. A conducting fluid traveling across a magnetic field interacts

with the field to produce MHD processes. Consequently, when a fluid flows across a transverse magnetic field, an electromagnetic force is generated. As a result, the fluid's movement is resisted by a combination of the magnetic field and current. Additionally, by producing its own magnetic field, the current warps the initial magnetic field. Applying an electric field perpendicular to the magnetic field is one method of creating a pumping or opposing force on the fluid. MHD waves, as well as upstream and downstream wave phenomena, can be caused by disturbances in the fluid or the magnetic field that propagates across both. The in-depth investigation of these phenomena, which also occur in nature and are generated by technological devices, is the science of MHD.

The fluid constituents' local structure and micro-motions create tiny effects in a class of fluids known as MPF. These fluids are made of a diluted suspension of stiff macromolecules that move independently to sustain stress and body moments under the effect of spin inertia. The presence of rotating micro-constituents in MPF can alter the flow's hydrodynamics and cause it to become noticeably non-Newtonian. A lot of research has been done on the dynamics of MPF because of Eringen's theory [1]. The impact of local rotating inertia and coupled pressures from realistic micro-rotation action are considered in this theory. Liquid crystals, suspensions, turbulence, and polymeric fluids are all covered under this theory. Numerous applications in the physical world and engineering have made this phenomenon well-known. The movement of a MPF through a stretching wall was examined by Na and Pop [2]. A MPF contained in a stretched sheet was the subject of an investigation by Desseaux and Kelson [3]. Hady [4] investigated the heat transfer (HT) solution including injection from a non-isothermal stretched sheet to a MPF. Convective HT in an electrically conducting MPF at a stretching surface with a uniform free stream was studied by researchers Abo-Eldahab and Ghonaim [5]. Mohammadein and Gorla [6] investigated viscous dissipation, internal heat generation, and a prescribed uniform surface temperature or wall heat flux in a laminar boundary layer of a MPF across a linearly stretched sheet. However, the effect of a magnetic field on the MPF problem has attracted a lot of attention lately. A numerical analysis of the boundary layer of a horizontal plate submerged in a MPF was provided by Mohammadein and Gorla [7]. Heat transport was examined in the presence of a magnetic field that caused buoyant stream wise pressure gradients and vectored surface mass transfer. They looked into how surface friction and HT rates were affected by buoyancy, material properties, mass transfer, and magnetic field. The Hall effect is the creation of a magnetic field perpendicular to the electric current flowing through an electrical conductor when the current is transverse to a voltage differential (the Hall voltage). Small magnetic fields are barely affected by the Hall term when Ohm's law is applied. The analysis of the impact of large magnetic fields on the flow of electrically conducting fluid, given by Sutton and Sherman [8], however, reveals that the electromagnetic force has an audible effect and induces anisotropic electrical conductivity in the plasma. Because of the plasma's anisotropic electrical conductivity, the Hall current travels through it. When the magnetic field is strong or the collision frequency is low, the Hall effect acts, producing a substantial Hall parameter. Other technical applications, including MHD power production, MHD accelerators, laboratory plasma flows, and other astronomical and geophysical scenarios, depend on how Hall current affects fluid flow and HT in spinning channels. The impact of Hall current on MHD flow in parallel plate channels in a rotating system has thus been studied by numerous researchers. The effects of Hall current on MHD Couette flow between parallel plates in a

rotating system were examined by Mandal & Mandal [9] and Ghosh [10]. Hydromagnetic convection in a rotating fluid layer with Hall current was investigated by Raghavachar and Gothandaraman [11]. Ghosh and Bhattacharjee [12] investigated the effects of Hall on MHD flow in a revolving channel when an inclined magnetic field was present. The unsteady flow of a non-Newtonian fluid in a rotating apparatus in relation to Hall current effects was examined by Hayat et al. [13]. Ghosh et al. [14] examined the impact of Hall effects on HT and MHD flow in a rotating channel. Using an infinite vertical porous plate, Arifuzzaman et al. [15] investigated the high order chemically reactive MPF. It has been demonstrated that vortices affect many facets, including energy production, transportation, environmental preservation, and medical advancements. Therefore, one of the most notable aspects of scientific and technical research in these areas is the capacity to predict, control, and optimize such vortices. Encouraged by all those possible uses, Ahmad et al. [16] have introduced a study to uncover the significance of vortices in MPF. Their findings indicate that at a certain Re, magnetic number, M causes a reduction of 45% in the $Nu$and a decline of one percent in the skin friction coefficient ($C_f Re$). The Nu and $C_f Re$, however, rise when the Re is raised at a constant M. It implies that an elevated velocity results in enhanced thermal transfer and wall shear stress, which destabilizes the flow and could lead to turbulence. An analysis of thermal radiation, chemical reaction, hall and ion slip effects on MHD oscilatory rotating MPFF has been performed by M. Veera krishna et al. [17] and their analysis let us know that raising the hall and ion slip factors causes the velocity and micro-rotation characteristics to grow, however raising the viscosity ratio and chemical reaction parameter has the opposite effect. The distributions of temperatures are supposed to rise with the thermal emission variable, however the opposite is seen as the oscillation frequency rises. Additionally, the concentration rises as the chemical reaction parameter increases and falls as the Schmidt number increases. A very recent investigation of MPF over a permeable stretching sheet is done by Kumar et al. [18] and they reveal that as couple stress increases, the velocity and temperature profiles get better; micro-rotation gets worse; velocity minimizes due to rising porosity; and concentration drops as Schmidt number and chemical reaction variables rise. Jalili et al [19] discovered in their study that as the magnetic parameter rose, the velocity profile and micro-rotation velocity also rose. Moreover, raising the rotation parameter raises the velocity. Additionally, the Pr and Brownian motion have a direct impact on the temperature profile, while the Re and Sc have an opposite effect. According to other findings, raising the Reynolds number, Re and thermophoretic

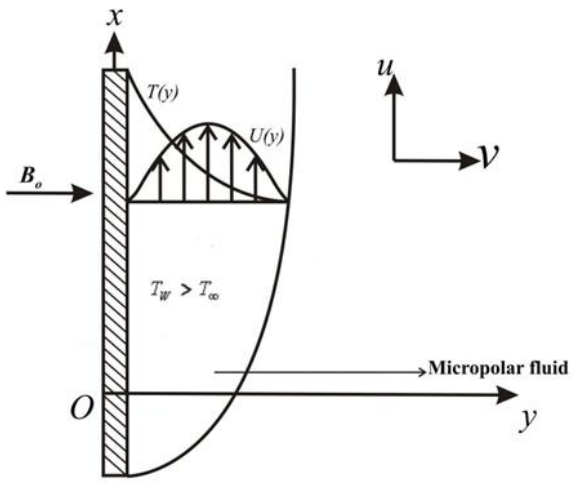

Fig.1 Physical Configuration and Co-ordinate System

parameter causes the concentration value to decrease. The substantial effect of the Hall current on flow characteristics, which improves velocity fields and changes the heat source's appearance [20]. Additionally, the study demonstrates that a heat source raises temperature fields and velocity, especially in micro-rotational profiles and the magnetic parameter accelerates micro-rotation, while vortex viscosity (Λ), which exhibits distinct characteristics from linear velocity, increases velocity with specific temperature and concentration.

Our main goal is therefore to investigate how the suction parameter affects HT on an infinite vertical plate that is transporting an unstable MPF. The model has been solved using the explicit finite difference method. A detailed examination of the temperature, velocity, and angular velocity over the boundary layer is presented and the corresponding graphs are shown.

2. Mathematical model

This study examines the unstable two-dimensional (plane) free convection of a MPF with HT flow, residing in a semi-infinite area of space enclosed by an infinite vertical limiting space. The heated plate is followed along the x-axis in an upward direction, and the y-axis is taken normal to it. A MPF with a temperature of T is present in the plate. In the transverse direction of the flow, a magnetic field of uniform strength B is applied. In order for the induced magnetic field to be ignored in comparison to the applied magnetic field and for $B = (0, B_0, 0)$ to occur, where B_0 is the uniform magnetic field acting normal to the plate, the flow's magnetic Reynolds number is assumed to be small enough. In Figure 1, the flow arrangement and coordinate system are displayed. With the Boussinesq approximation applied, the flow of an unstable incompressible MPF can be expressed as follows:

Momentum Equation:

$$\frac{\partial u}{\partial t} + u\frac{\partial u}{\partial x} + v\frac{\partial u}{\partial y} = \left(\upsilon + \frac{\chi}{\rho}\right)\frac{\partial^2 u}{\partial y^2} + \frac{\chi}{\rho}\frac{\partial \Omega}{\partial y} + g\beta(T - T_\infty) - \frac{1}{\rho}\frac{B_0^2\sigma_e}{(1+m^2)}(wm + u)\sin^2\left(\frac{\pi x}{\upsilon}\right) \quad (1)$$

$$\frac{\partial w}{\partial t} + u\frac{\partial w}{\partial x} + v\frac{\partial w}{\partial y} = \left(\upsilon + \frac{\chi}{\rho}\right)\frac{\partial^2 w}{\partial y^2} + \frac{1}{\rho}\frac{B_0^2\sigma_e}{(1+m^2)}(um - w) \quad (2)$$

Angular momentum Equation:

$$\frac{\partial \Omega}{\partial t} + u\frac{\partial \Omega}{\partial x} + v\frac{\partial \Omega}{\partial y} = \frac{\gamma}{\rho j}\frac{\partial^2 \Omega}{\partial y^2} - \frac{\chi}{\rho j}\left(2\Omega + \frac{\partial u}{\partial y}\right) \quad (3)$$

Energy Equation:

$$\frac{\partial T}{\partial t} + u\frac{\partial T}{\partial x} + v\frac{\partial T}{\partial y} = \frac{k}{\rho c_p}\frac{\partial^2 T}{\partial y^2} + \frac{1}{c_p}\left(\upsilon + \frac{\chi}{\rho}\right)\left(\frac{\partial u}{\partial y}\right)^2 \quad (4)$$

Initial and boundary conditions are

$$t \le 0, \quad u = 0, \quad w = 0, \quad \Omega = 0, \quad T \to T_\infty \quad \text{every where} \quad (5)$$

$$\left.\begin{array}{lllll} & u = 0, & w = 0, & \Omega = 0, & T \to T_\infty \quad \text{at } x = 0 \\ t > 0, & u = 0, & w = 0, & \Omega = -s\dfrac{\partial u}{\partial y}, & T = T_w \quad \text{at } y = 0 \\ & u = 0, & w = 0, & \Omega = 0, & T \to T_\infty \quad \text{as } y \to \infty \end{array}\right\} \quad (6)$$

where the velocity components in the x, y and z directions are u, v and w, respectively, g represents the acceleration due to gravity, ρ indicates the density, υ represents the kinematic viscosity, β identifies the coefficient of volume expansion. The fluid temperature in the free stream, the plate temperature, and the fluid temperature inside the thermal boundary layer are denoted by the letters T, T_w and T_∞. Additionally k represents the thermal conductivity of the medium, C_p symbolize the specific heat at constant pressure, Ω be the micro-rotation component, σ_e indicates the electrical conductivity, γ declare the spin gradient viscosity, χ represents the vortex viscosity, j indicates the micro-inertia per unit mass and other symbols have their usual meaning. s be an arbitrary constant. Since the microelements in a concentrated particle flow near the wall are unable to rotate, we obtain $G = 0$ for $s = 0$, which denotes the no-spin condition. The scenario $s = 1/2$ denotes weak concentration and the vanishing of the stress tensor's anti-symmetric portion. At the wall, the fluid velocity equals the particle spin in a suspension of small particles. An example of turbulent boundary layer flow is the case $s = 1$.

3. Mathematical framework

The governing equations (1)–(4) must be made dimensionless since the finite difference method will be used to solve them under the initial circumstances (5) and the boundary conditions (6). The following dimensionless quantities are newly introduced for this purpose:

$$X = \frac{xU_o}{\upsilon}, Y = \frac{yU_o}{\upsilon}, U = \frac{u}{U_o}, V = \frac{v}{U_o}, W = \frac{w}{U_o}, \tau = \frac{tU_o^2}{\upsilon}, \Gamma = \frac{\Omega\upsilon}{U_o^2}, \theta = \frac{T - T_\infty}{T_w - T_\infty}$$

With regard to dimensionless variables, the following nonlinear coupled PDEs are obtained:

$$\frac{\partial U}{\partial \tau} + U\frac{\partial U}{\partial X} + V\frac{\partial U}{\partial Y} = (1+\Delta)\frac{\partial^2 U}{\partial Y^2} + \Delta\frac{\partial \Gamma}{\partial Y} + G_r\theta - \frac{M}{1+m^2}\sin^2(\pi X)\,(U + mW) \tag{7}$$

$$\frac{\partial W}{\partial \tau} + U\frac{\partial W}{\partial X} + V\frac{\partial W}{\partial Y} = (1+\Delta)\frac{\partial^2 W}{\partial Y^2} + \frac{M}{1+m^2}(mU - W) \tag{8}$$

$$\frac{\partial \Gamma}{\partial \tau} + U\frac{\partial \Gamma}{\partial X} + V\frac{\partial \Gamma}{\partial Y} = \Lambda\frac{\partial^2 \Gamma}{\partial Y^2} - \lambda\left(2\Gamma + \frac{\partial U}{\partial Y}\right) \tag{9}$$

$$\frac{\partial \theta}{\partial \tau} + U\frac{\partial \theta}{\partial X} + V\frac{\partial \theta}{\partial Y} = \frac{1}{\mathrm{P_r}}\frac{\partial^2 \theta}{\partial Y^2} + (1+\Delta)E_c\left(\frac{\partial U}{\partial Y}\right)^2 \tag{10}$$

with the matching beginning and boundary conditions being

$$\tau \le 0, \quad U = 0, \quad W = 0, \quad \Gamma = 0, \quad \theta = 0 \quad \text{every where} \tag{11}$$

$$\left.\begin{array}{llll} U = 0, & W = 0, & \Gamma = 0, & \theta = 0 \quad \text{at } X = 0 \\ \tau > 0, \quad U = 0, & W = 0, & \Gamma = -s\dfrac{\partial U}{\partial Y}, & \theta = 1 \quad \text{at } Y = 0 \\ U = 0, & W = 0, & \Gamma = 0, & \theta = 0 \quad \text{as } Y \to \infty \end{array}\right\} \tag{12}$$

where $G_r, \lambda, \Lambda, M, P_r, \Delta, E_c$ and s stand for the Grashof number, spin gradient viscosity, vortex viscosity, magnetic parameter, Prandlt number, microrotation number, Eckert number and suction parameter respectively.

4. Numerical solutions

In this section, we attempt to solve the governing second order nonlinear coupled dimensionless partial differential equations with the associated initial and boundary conditions. From the concept of the above discussion, for simplicity the explicit finite difference method has been used to solve equations $(7)-(10)$ subject to the conditions given by (11) and (12). To obtain the difference equations the region of the flow is divided into a grid or mesh of lines parallel to X and Y axes where X-axis is taken along the plate and Y-axis is normal to the plate.

Here we consider that the plate of height $X_{max}(=100)$ i.e. X varies from 0 to 100 and regard $Y_{max}(=25)$ as corresponding to $Y\to\infty$ i.e.Y varies from 0 to 25. There are $m=100$ and $n=100$ grid spacings in the X and Y directions respectively as shown in Figure. 2.

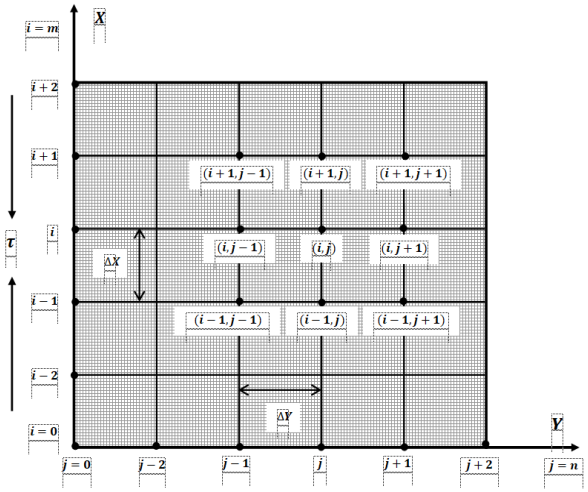

Fig. 2. Finite difference space grid.

It is assumed that ΔX, ΔY are constant mesh sizes along X and Y directions respectively and taken as follows,

$$\Delta X = 1.00(0 \le x \le 100)$$
$$\Delta Y = 0.25(0 \le y \le 25)$$

with the smaller time-step, $\Delta\tau = 0.005$

Let $\acute{U}$, $\acute{V}$, $\acute{W}$, $\acute{\Gamma}$ & $\acute{\theta}$ denote the values of U, V, W, Γ & θ at the end of a time-step respectively. Using the explicit finite difference approximation we have,

$$\left(\frac{\partial U}{\partial \tau}\right)_{i,j} = \frac{\acute{U}_{i,j} - U_{i,j}}{\Delta\tau}, \quad \left(\frac{\partial U}{\partial X}\right)_{i,j} = \frac{U_{i,j} - U_{i-1,j}}{\Delta X}, \quad \left(\frac{\partial U}{\partial Y}\right)_{i,j} = \frac{U_{i,j+1} - U_{i,j}}{\Delta Y}$$

$$\left(\frac{\partial V}{\partial Y}\right)_{i,j} = \frac{V_{i,j} - V_{i,j-1}}{\Delta Y}, \quad \left(\frac{\partial W}{\partial \tau}\right)_{i,j} = \frac{\acute{W}_{i,j} - W_{i,j}}{\Delta\tau}, \quad \left(\frac{\partial W}{\partial X}\right)_{i,j} = \frac{W_{i,j} - W_{i-1,j}}{\Delta X}$$

$$\left(\frac{\partial W}{\partial Y}\right)_{i,j} = \frac{W_{i,j+1} - W_{i,j}}{\Delta Y}, \quad \left(\frac{\partial \Gamma}{\partial \tau}\right)_{i,j} = \frac{\acute{\Gamma}_{i,j} - \Gamma_{i,j}}{\Delta\tau}, \quad \left(\frac{\partial \Gamma}{\partial X}\right)_{i,j} = \frac{\Gamma_{i,j} - \Gamma_{i-1,j}}{\Delta X}$$

$$\left(\frac{\partial \Gamma}{\partial Y}\right)_{i,j} = \frac{\Gamma_{i,j+1} - \Gamma_{i,j}}{\Delta Y}, \quad \left(\frac{\partial \theta}{\partial \tau}\right)_{i,j} = \frac{\acute{\theta}_{i,j} - \theta_{i,j}}{\Delta\tau}, \quad \left(\frac{\partial \theta}{\partial X}\right)_{i,j} = \frac{\theta_{i,j} - \theta_{i-1,j}}{\Delta X}$$

$$\left(\frac{\partial \theta}{\partial Y}\right)_{i,j} = \frac{\theta_{i,j+1} - \theta_{i,j}}{\Delta Y}, \quad \left(\frac{\partial^2 U}{\partial Y^2}\right)_{i,j} = \frac{U_{i,j+1} - 2U_{i,j} + U_{i,j-1}}{(\Delta Y)^2}$$

$$\left(\frac{\partial^2 W}{\partial Y^2}\right)_{i,j} = \frac{W_{i,j+1} - 2W_{i,j} + W_{i,j-1}}{(\Delta Y)^2}, \quad \left(\frac{\partial^2 \Gamma}{\partial Y^2}\right)_{i,j} = \frac{\Gamma_{i,j+1} - 2\Gamma_{i,j} + \Gamma_{i,j-1}}{(\Delta Y)^2}$$

$$\left(\frac{\partial^2 \theta}{\partial Y^2}\right)_{i,j} = \frac{\theta_{i,j+1} - 2\theta_{i,j} + \theta_{i,j-1}}{(\Delta Y)^2}$$

From the system of partial differential equations $(7)-(10)$ with substituting the above relations into the corresponding differential equation we obtain an appropriate set of finite difference equations,

$$\frac{\acute{U}_{i,j}-U_{i,j}}{\Delta\tau}+U_{i,j}\frac{U_{i,j}-U_{i-1,j}}{\Delta X}+V_{i,j}\frac{U_{i,j+1}-U_{i,j}}{\Delta Y}$$
$$=(1+\Delta)\frac{U_{i,j+1}-2U_{i,j}+U_{i,j-1}}{(\Delta Y)^2}+G_r\theta_{i,j}$$
$$+\frac{\Gamma_{i,j+1}-\Gamma_{i,j}}{\Delta Y}-\frac{M}{1+m^2}\sin^2(\pi X)\left(U_{i,j}+mW_{i,j}\right) \quad (13)$$

$$\frac{\acute{W}_{i,j}-W_{i,j}}{\Delta\tau}+U_{i,j}\frac{W_{i,j}-W_{i-1,j}}{\Delta X}+V_{i,j}\frac{W_{i,j+1}-W_{i,j}}{\Delta Y}=(1+\Delta)\frac{W_{i,j+1}-2W_{i,j}+W_{i,j-1}}{(\Delta Y)^2}$$
$$+\frac{M}{1+m^2}\left(mU_{i,j}-W_{i,j}\right) \quad (14)$$

$$\frac{\acute{\Gamma}_{i,j}-\Gamma_{i,j}}{\Delta\tau}+U_{i,j}\frac{\Gamma_{i,j}-\Gamma_{i-1,j}}{\Delta X}+V_{i,j}\frac{\Gamma_{i,j+1}-\Gamma_{i,j}}{\Delta Y}=\Lambda\frac{\Gamma_{i,j+1}-2\Gamma_{i,j}+\Gamma_{i,j-1}}{(\Delta Y)^2}$$
$$-\lambda\left(2\Gamma_{i,j}+\frac{U_{i,j+1}-U_{i,j}}{\Delta Y}\right) \quad (15)$$

$$\frac{\acute{\theta}_{i,j}-\theta_{i,j}}{\Delta\tau}+U_{i,j}\frac{\theta_{i,j}-\theta_{i-1,j}}{\Delta X}+V_{i,j}\frac{\theta_{i,j+1}-\theta_{i,j}}{\Delta Y}=\frac{1}{P_r}\frac{\theta_{i,j+1}-2\theta_{i,j}+\theta_{i,j-1}}{(\Delta Y)^2}$$
$$+(1+\Delta)E_c\left(\frac{U_{i,j+1}-U_{i,j}}{\Delta Y}\right)^2 \quad (16)$$

Corresponding initial and boundary conditions are

$$U_{i,j}^0=0 \qquad w_{i,j}^0=0 \qquad \Gamma_{i,j}^0=0 \qquad \theta_{i,j}^0=0 \quad (17)$$
$$U_{0,j}^n=0 \qquad w_{0,j}^n=0 \qquad \Gamma_{0,j}^n=0 \qquad \theta_{0,j}^n=0$$

$$U_{i,0}^n=0 \qquad w_{i,0}^n=0 \qquad \Gamma_{i,0}^n=-s\frac{U^n{}_{i,j+1}-U^n{}_{i,j}}{\Delta Y} \qquad \theta_{i,0}^n=1 \quad (18)$$
$$U_{i,L}^n=0 \qquad w_{i,L}^n=0 \qquad \Gamma_{i,L}^n=0 \qquad \theta_{i,L}^n=0 \quad where, L\to\infty$$

Here the subscripts i and j designate the grid points with x and y coordinates respectively and the superscript n represents a value of time, $\tau=n\Delta\tau$ where $n=0,1,2,3,\ldots..$ From the initial condition (17), the values of U, W, Γ and θ are known at $\tau=0$. During any one time-step, the coefficients $U_{i,j}$ and $V_{i,j}$ appearing in equations $(13)-(16)$ are treated as constants. Then at the end of any time-step $\Delta\tau$, the new angular velocity $\acute{\Gamma}$, the new temperature $\acute{\theta}$, the new primary velocity $\acute{U}$, the new secondary velocity $\acute{W}$ at all interior nodal points may be obtained by successive applications of equations $(15),(16),(13),$ and (14) respectively. This process is repeated in time and provided the time-step is sufficiently small, U, V, W, Γ & θ should eventually converge to values which approximate the steady-state solution of equations $(7)-(10)$. The numerical values of the Shear stress, Couple shear stress and Nusselt number are evaluated by a five-point approximate formula for the derivative, and then the average Shear Stress, Couple stress and Nusselt number are calculated by the use of Simpson's 1/3 integration formula. These converged solutions are shown graphically in Figure 3 to Figure 22.

5. Stability and convergence analysis

Since an explicit procedure is being used, the analysis will remain incomplete unless we discuss the stability and convergence of the finite difference scheme**.** For the constant mesh sizes the stability criteria of the scheme may be established as follows:

The general terms of the Fourier expansion for $U,\ W,\ \Gamma\ \&\ \theta$ at a time arbitrarily called $t = 0$ are all $e^{i\alpha X}e^{i\beta Y}$, apart from a constant, where $i = \sqrt{-1}$. At a time $t = \tau$, these terms become

$$\left.\begin{array}{ll} U: & \psi(\tau)e^{i\alpha X}e^{i\beta Y} \\ W: & \phi(\tau)e^{i\alpha X}e^{i\beta Y} \\ \Gamma: & \gamma(\tau)e^{i\alpha X}e^{i\beta Y} \\ \theta: & \Theta(\tau)e^{i\alpha X}e^{i\beta Y} \end{array}\right\} \tag{19}$$

and after the time-step these terms will become

$$\left.\begin{array}{ll} \acute{U}: & \acute{\psi}(\tau)e^{i\alpha X}e^{i\beta Y} \\ \acute{W}: & \acute{\phi}(\tau)e^{i\alpha X}e^{i\beta Y} \\ \acute{\Gamma}: & \acute{\gamma}(\tau)e^{i\alpha X}e^{i\beta Y} \\ \acute{\theta}: & \acute{\Theta}(\tau)e^{i\alpha X}e^{i\beta Y} \end{array}\right\} \tag{20}$$

Substituting (19) and (20) into equations $(13) - (16)$, regarding the coefficients U and V as constants over any one time-step, we obtain the following equations upon simplification,

$$\frac{\acute{\psi}(\tau) - \psi(\tau)}{\Delta\tau} + U\frac{\psi(\tau)\left(1 - e^{-i\alpha\Delta X}\right)}{\Delta X} + V\frac{\psi(\tau)\left(e^{i\beta\Delta Y} - 1\right)}{\Delta Y} = G_r\acute{\Theta}(\tau) +$$
$$(1+\Delta)\frac{2\psi(\tau)(cos\beta\Delta Y - 1)}{(\Delta Y)^2} + \Delta\frac{\gamma(\tau)\left(e^{i\beta\Delta Y} - 1\right)}{\Delta Y} - \frac{M}{1+m^2}\left(\psi(\tau) + m\phi(\tau)\right) \tag{21}$$

$$\frac{\acute{\phi}(\tau) - \phi(\tau)}{\Delta\tau} + U\frac{\phi(\tau)\left(1 - e^{-i\alpha\Delta X}\right)}{\Delta X} + V\frac{\phi(\tau)\left(e^{i\beta\Delta Y} - 1\right)}{\Delta Y} =$$
$$(1+\Delta)\frac{2\phi(\tau)(cos\beta\Delta Y - 1)}{(\Delta Y)^2} + \frac{M}{1+m^2}\left(m\psi(\tau) - \phi(\tau)\right) \tag{22}$$

$$\frac{\acute{\gamma}(\tau) - \gamma(\tau)}{\Delta\tau} + U\frac{\gamma(\tau)\left(1 - e^{-i\alpha\Delta X}\right)}{\Delta X} + V\frac{\gamma(\tau)\left(e^{i\beta\Delta Y} - 1\right)}{\Delta Y} =$$
$$\Lambda\frac{2\gamma(\tau)(cos\beta\Delta Y - 1)}{(\Delta Y)^2} - \lambda\left\{2\gamma(\tau) + \frac{\psi(\tau)\left(e^{i\beta\Delta Y} - 1\right)}{\Delta Y}\right\} \tag{23}$$

$$\frac{\acute{\Theta}(\tau) - \Theta(\tau)}{\Delta\tau} + U\frac{\Theta(\tau)\left(1 - e^{-i\alpha\Delta X}\right)}{\Delta X} + V\frac{\Theta(\tau)\left(e^{i\beta\Delta Y} - 1\right)}{\Delta Y} =$$
$$\frac{1}{P_r}\frac{2\Theta(\tau)(cos\beta\Delta Y - 1)}{(\Delta Y)^2} + (1+\Delta)E_c\left\{\frac{\psi(\tau)\left(e^{i\beta\Delta Y} - 1\right)}{\Delta Y}\right\} \tag{24}$$

The equations (21), (22), (23) and (24) can be written in the following form

$$\acute{\psi} = A\psi + B\phi + C\gamma + \mathrm{D}\Theta \tag{25}$$
$$\acute{\phi}(\tau) = E\phi + F\psi \tag{26}$$
$$\acute{\gamma}(\tau) = G\gamma + H\psi \tag{27}$$
$$\acute{\Theta}(\tau) = I\Theta + \mathrm{J}\psi \tag{28}$$

where

$$A = 1 - U\frac{\Delta\tau}{\Delta X}\left(1 - e^{-i\alpha\Delta X}\right) - V\frac{\Delta\tau}{\Delta Y}\left(e^{i\beta\Delta Y} - 1\right) + (1+\Delta)\frac{2\Delta\tau}{(\Delta Y)^2}(cos\beta\Delta Y - 1) - \frac{M}{1+m^2}\Delta\tau$$

$$B = -\frac{Mm}{1+m^2}\Delta\tau, C = \Delta\frac{\Delta\tau}{\Delta Y}\left(e^{i\beta\Delta Y} - 1\right), D = G_r\Delta\tau$$

$$E = 1 - U\frac{\Delta\tau}{\Delta X}\left(1 - e^{-i\alpha\Delta X}\right) - V\frac{\Delta\tau}{\Delta Y}\left(e^{i\beta\Delta Y} - 1\right) + (1+\Delta)\frac{2\Delta\tau}{(\Delta Y)^2}(cos\beta\Delta Y - 1) - \frac{M}{1+m^2}$$

$$F = \frac{Mm}{1+m^2}, G = 1 - U\frac{\Delta\tau}{\Delta X}\left(1 - e^{-i\alpha\Delta X}\right) - V\frac{\Delta\tau}{\Delta Y}\left(e^{i\beta\Delta Y} - 1\right) + \Lambda\frac{2\Delta\tau}{(\Delta Y)^2}(cos\beta\Delta Y - 1) - 2\lambda\Delta\tau$$

$$H = -\lambda\frac{\Delta\tau}{\Delta Y}\left(e^{i\beta\Delta Y} - 1\right),$$

$$I = 1 - U\frac{\Delta\tau}{\Delta X}\left(1 - e^{-i\alpha\Delta X}\right) - V\frac{\Delta\tau}{\Delta Y}\left(e^{i\beta\Delta Y} - 1\right) + \frac{1}{\mathrm{P_r}}\frac{2\Delta\tau}{(\Delta Y)^2}(cos\beta\Delta Y - 1)$$

$$J = (1+\Delta)E_c\frac{\Delta\tau}{(\Delta Y)^2}\left(e^{i\beta\Delta Y} - 1\right)^2$$

and these equations $(25) - (28)$ are expressed in matrix notation,

$$\begin{bmatrix}\acute{\psi}\\ \acute{\phi}\\ \acute{\gamma}\\ \acute{\Theta}\end{bmatrix} = \begin{bmatrix}A & B & C & D\\ F & E & 0 & 0\\ H & 0 & G & 0\\ J & 0 & 0 & I\end{bmatrix}\begin{bmatrix}\psi\\ \phi\\ \gamma\\ \Theta\end{bmatrix} \tag{29}$$

that is, $\acute{\eta} = T\eta$

where $\acute{\eta} = \begin{bmatrix}\acute{\psi}\\ \acute{\phi}\\ \acute{\gamma}\\ \acute{\Theta}\end{bmatrix}$, $T = \begin{bmatrix}A & B & C & D\\ F & E & 0 & 0\\ H & 0 & G & 0\\ J & 0 & 0 & I\end{bmatrix}$ and $\eta = \begin{bmatrix}\psi\\ \phi\\ \gamma\\ \Theta\end{bmatrix}$

For obtaining the stability condition we have to find out eigenvalues of the amplification matrix T but this study is very difficult since it is a fourth order square matrix and all the elements of T are different. Hence the problem requires that the Eckert Number E_c is assumed to be very small that is tends to zero. Under this consideration we have $J = 0$ and the amplification matrix becomes

$$T = \begin{bmatrix}A & B & C & D\\ F & E & 0 & 0\\ H & 0 & G & 0\\ 0 & 0 & 0 & I\end{bmatrix}$$

After simplification of the matrix T we get,

$$\begin{bmatrix}A & B & C & D\\ F & E & 0 & 0\\ H & 0 & G & 0\\ 0 & 0 & 0 & I\end{bmatrix} - \begin{bmatrix}\lambda & 0 & 0 & 0\\ 0 & \lambda & 0 & 0\\ 0 & 0 & \lambda & 0\\ 0 & 0 & 0 & \lambda\end{bmatrix} = 0, \Longrightarrow \begin{bmatrix}A-\lambda & B & C & D\\ F & E-\lambda & 0 & 0\\ H & 0 & G-\lambda & 0\\ 0 & 0 & 0 & I-\lambda\end{bmatrix} = 0$$

$$\Longrightarrow \{(A-\lambda)(E-\lambda) - BF\}(G-\lambda)(I-\lambda) = 0$$

So the eigenvalues are $\lambda_1 = G,\ \lambda_2 = I$ And

$(A-\lambda)(E-\lambda) - BF = 0$

$\Longrightarrow AE - \lambda A - \lambda E + \lambda^2 - BF = 0$

$\Longrightarrow \lambda^2 - (A+E)\lambda + AE - BF = 0$

$$\Longrightarrow \lambda = \frac{A+E \pm \sqrt{(A+E)^2 - (4AE - 4BF)}}{2}$$

$$\Longrightarrow \lambda = \frac{A+E \pm \sqrt{(A-E)^2 + 4BF}}{2}$$

$$\therefore \lambda_3 = \frac{A+E+\sqrt{(A-E)^2+4BF}}{2} \quad \text{and} \quad \lambda_4 = \frac{A+E-\sqrt{(A-E)^2+4BF}}{2}$$

For stability, each eigenvalue $\lambda_1,\ \lambda_2,\ \lambda_3\ and\ \lambda_4$ must not exceed unity in modulus. Hence the stability condition is

$$|G| \le 1, \qquad |I| \le 1, \qquad \left|\frac{A+E+\sqrt{(A-E)^2+4BF}}{2}\right| \le 1$$

and $$\left|\frac{A+E-\sqrt{(A-E)^2+4BF}}{2}\right| \le 1 \text{ for all } \alpha, \beta$$

Now we assume that U is everywhere nonnegative and V is everywhere nonpositive. Thus

$$G = (1-a-b-\Lambda 2c) + ae^{-i\alpha\Delta X} + be^{i\beta\Delta Y} + \Lambda 2c\, cos\beta\Delta Y - 2\lambda\Delta\tau$$

where, $a = U\frac{\Delta\tau}{\Delta X}$, $\quad b = |V|\frac{\Delta\tau}{\Delta Y}$ and $c = \frac{\Delta\tau}{(\Delta Y)^2}$

The coefficients a, b and c are all real and nonnegative. We can demonstrated that the maximum modulus of G occurs when $\alpha\Delta X = m\pi$ and $\beta\Delta Y = n\pi$, where m and n are integers and hence G is real. The value of $|G|$ is greater when both m and n are odd integers, in which case

$G = (1-a-b-\Lambda 2c) - a - b - \Lambda 2c\ - 2\lambda\Delta\tau$

$\Longrightarrow G = 1 - 2(a+b+\Lambda 2c + \lambda\Delta\tau)$

To satisfy the first condition $|G| \le 1$, the most negative allowable value is $G = -1$ Therefore the first stability condition is

$2(a+b+\Lambda 2c+\lambda\Delta\tau) \le 2$

that is,

$$U\frac{\Delta\tau}{\Delta X} + |V|\frac{\Delta\tau}{\Delta Y} + \Lambda\frac{2\Delta\tau}{(\Delta Y)^2} + \lambda\Delta\tau \le 1 \tag{30}$$

Likewise, the second condition $|J| \le 1$ requires that

$$U\frac{\Delta\tau}{\Delta X} + |V|\frac{\Delta\tau}{\Delta Y} + \frac{2}{\mathrm{P_r}}\frac{\Delta\tau}{(\Delta Y)^2} \le 1 \tag{31}$$

Hence the stability conditions of the problem are as furnished below

$$U\frac{\Delta\tau}{\Delta X} + |V|\frac{\Delta\tau}{\Delta Y} + \Lambda\frac{2\Delta\tau}{(\Delta Y)^2} + \lambda\Delta\tau \le 1 \tag{32}$$

$$U\frac{\Delta\tau}{\Delta X} + |V|\frac{\Delta\tau}{\Delta Y} + \frac{2}{\mathrm{P_r}}\frac{\Delta\tau}{(\Delta Y)^2} \le 1 \tag{33}$$

Since from the initial condition, $U = V = 0\ at\ \tau = 0$ so the equations (32) and (33) gives $P_r \ge 0.25$ and parameter Λ and λ depended arbitrary values of each other.

Hence the convergence criteria of the problem are $P_r \geq 0.25$ and Λ and λ depended different values of each other.

6. Results and discussion

For the purpose of discussing the results of the problem, the approximate solutions are obtained for various parameters with small values of Eckert number. In order to analyze the physical situation of the model, we have computed the steady state numerical values of the non-dimensional primary velocity U, secondary velocity W, angular velocity Γ and temperature θ within the boundary layer for different values of magnetic parameter(M), Grashof number(G_r), Prandtal number(P_r), Spin gradient viscosity (λ), Micro Rotation number (Δ), Vortex viscosity (Λ), Hall current (m) and Eckert number(E_c). The graphs are represented with some constant parameters $M = 2.0, m = 0.5, \Delta = 0.5, \Lambda = 1.0, \lambda = 0.10, E_c = 0.01, P_r = 1.0, G_r = 5.00, s = 0.05$. In the figure-3, the effect of primary velocity profiles has been shown for different data of M. It is examined that the field of velocity decreases for increasing M. The curve to curve fluctuation for velocity profiles diminishes $24.19\%, 20.97\%$ and 11.57% as M changes from 1.00 to 25.0 respectively at $\tau = 5.00$. Similarly in figure-4, velocity profiles are decreases when raises the values of P_r. Figures 5-6 describe that the increase of velocity profiles with respect to increasing the parameter values of G_r and m.

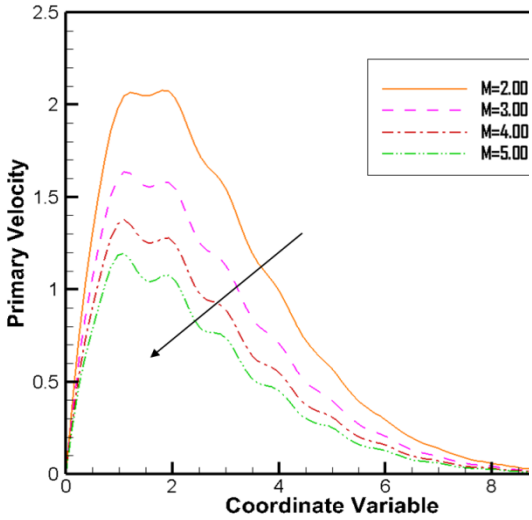

Figure 3: The impact of M on U

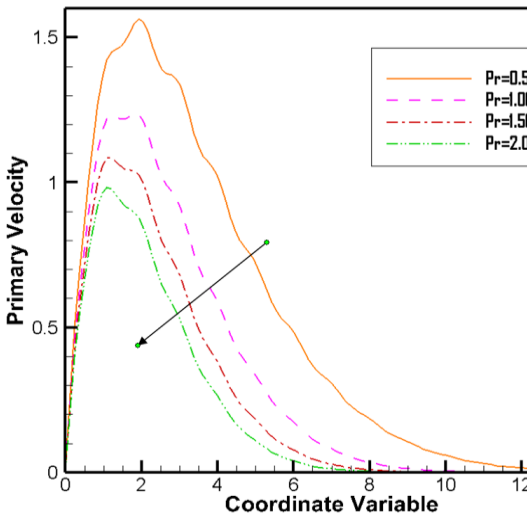

Figure 4: The impact of P_r on U

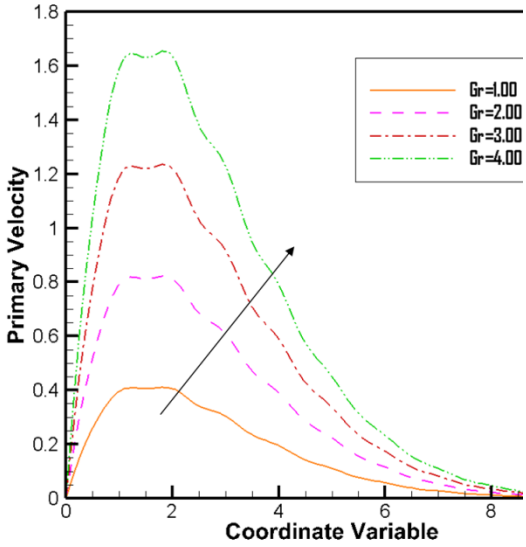

Figure 5: The impact of G_r on U

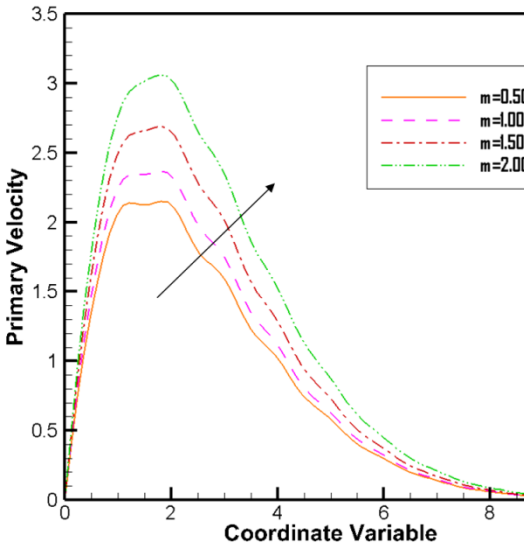

Figure 6: The impact of m on U

We discussed the effects of secondary velocity profile (SVP) for different parameter values in the Figures 7-10. The impression of M, P_r , G_r and m in secondary velocity field, we observed that the SVP decreases due to rising of M and P_r respectively in Figure 7 and Figure 8. Also in Figure 9 and Figure 10, SVP increases with the raise of G_r and m respectively. The angular velocity profiles (AVPs) are illustrated for different values of M, P_r , G_r and m. The AVP increases with the increase of M and P_r shown in Figures 11-12 and decreases with the increase of G_r and m which are shown in Figures 13 and Figure 14.

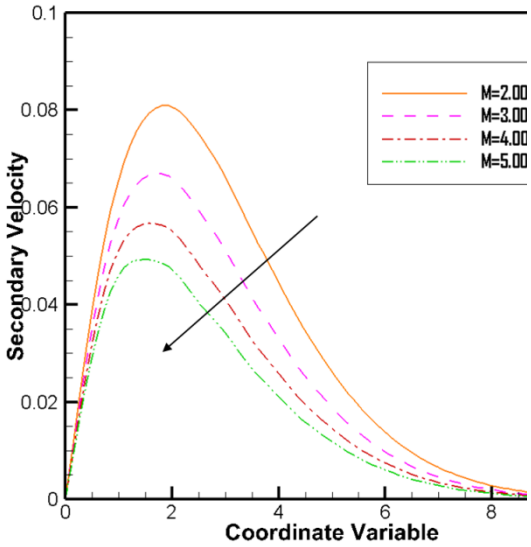

Figure 7: The impact of M on W

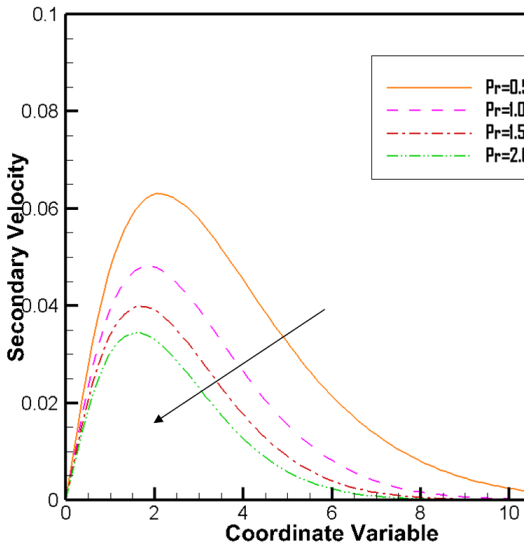

Figure 8: The impact of P_r on W

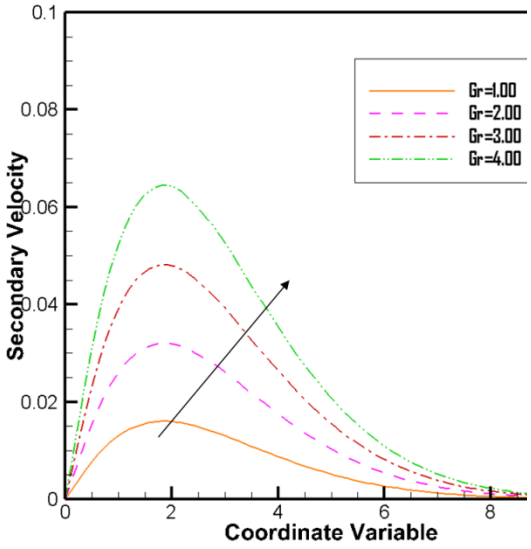

Figure 9: The impact of G_r on W

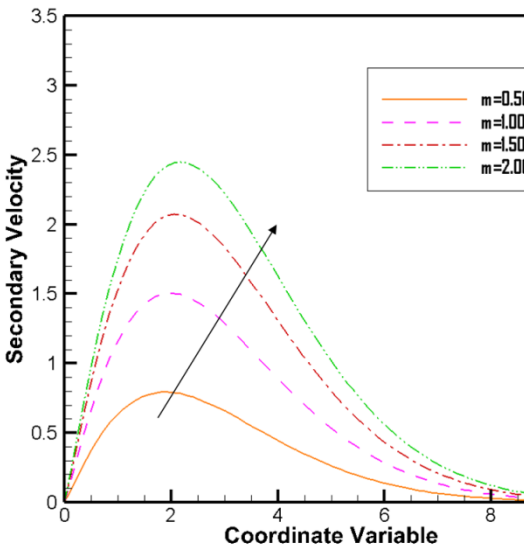

Figure 10: The impact of m on W

Now we analyzed the skin friction (Figures 15 to 18) and Nusselt number (Nu) (Figures 19 to 22) for different parameters data. From Figures 15 and 16, they are noticed to have an increase values of M and P_r in the reduction of the skin friction and fro the Figure 17 and Figure 18, we observed that the skin friction distribution increase with the increasing of G_r and m.

The MHD effects on Nu is illustrated in Figures 19 to 22. Figure 19 represented that the Nu profiles is detected to be increased for the increase of M and Figure 20, Figure 21 and Figure 22 which are illustrated Nu profiles decrease with the increase of P_r, G_r and m respectively.

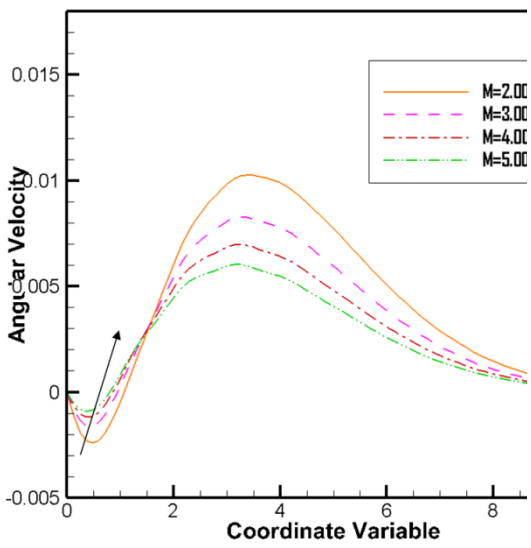

Figure 11: The impact of M on Γ

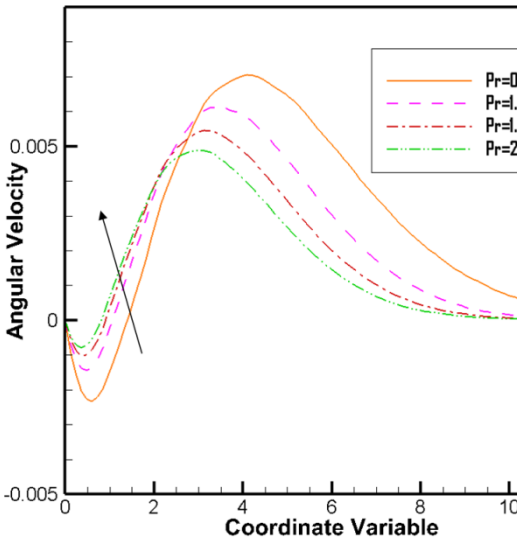

Figure 12: The impact of P_r on Γ

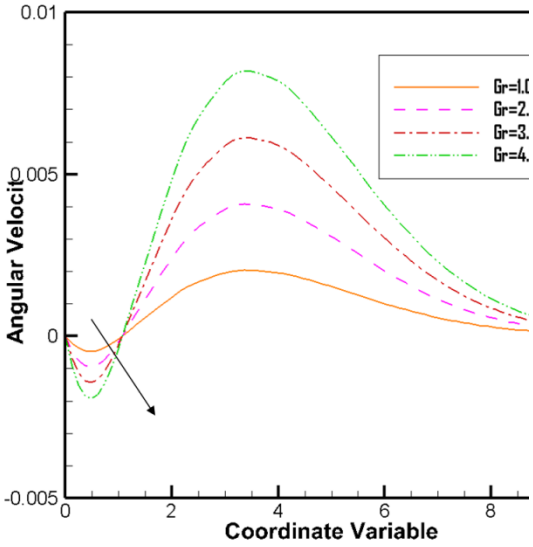

Figure 13: The impact of G_r on Γ

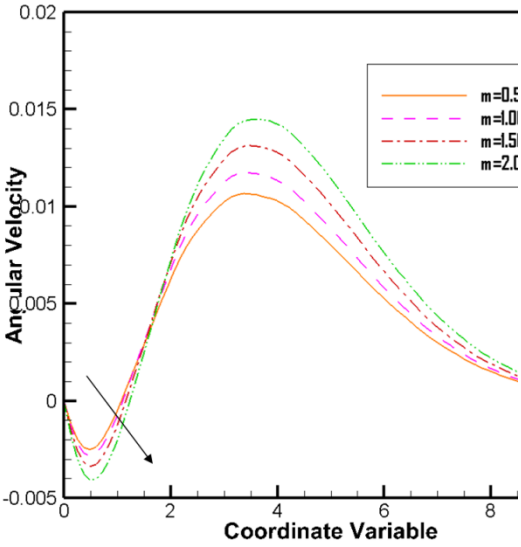

Figure 14: The impact of m on Γ

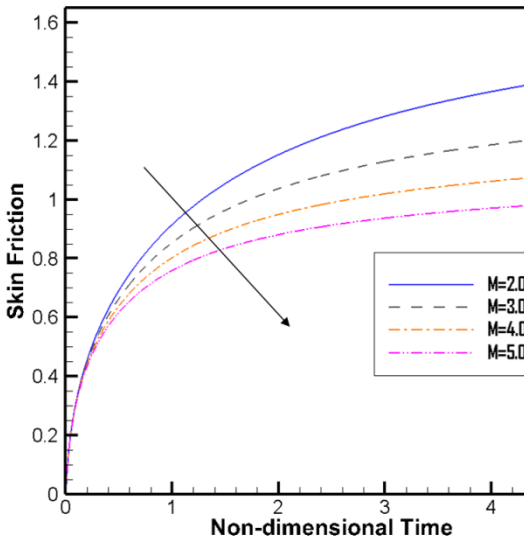

Figure 15: The impact of M on C_f

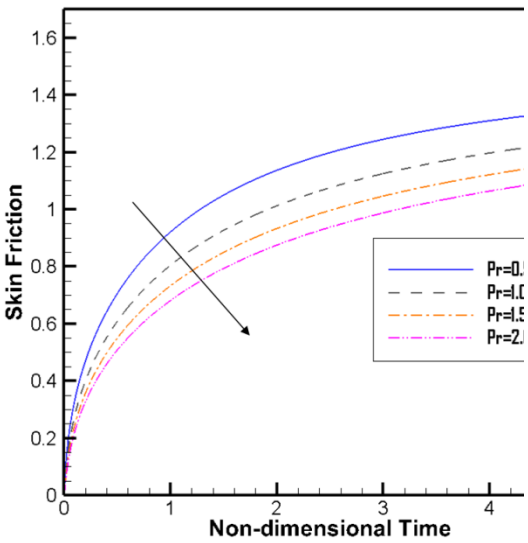

Figure 16: The impact of P_r on C_f

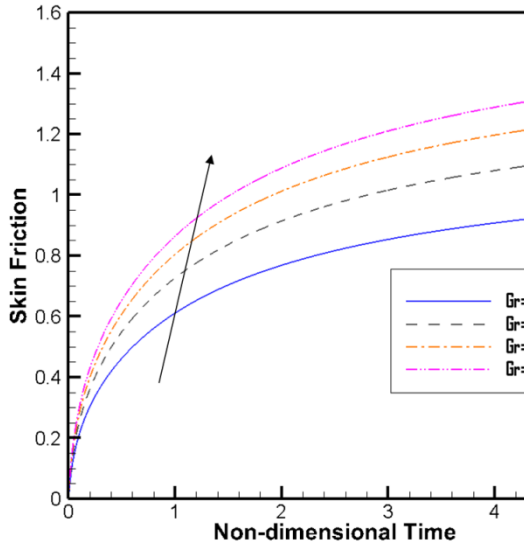

Figure 17: The impact of G_r on C_f

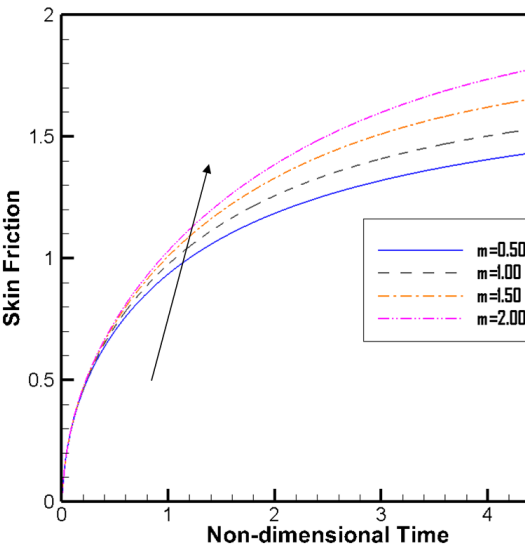

Figure 18: The impact of m on C_f

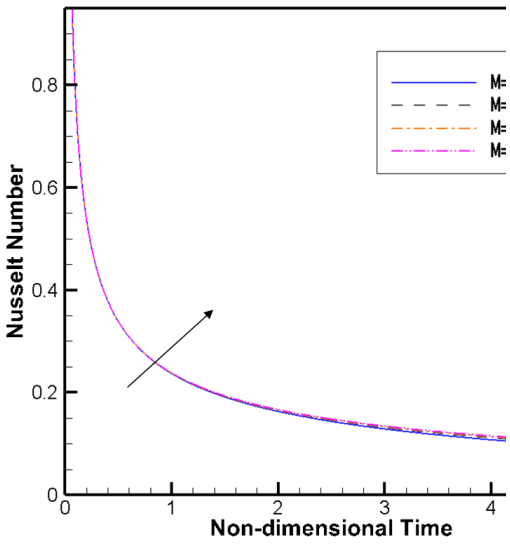

Figure 19: The impact of M on N_u

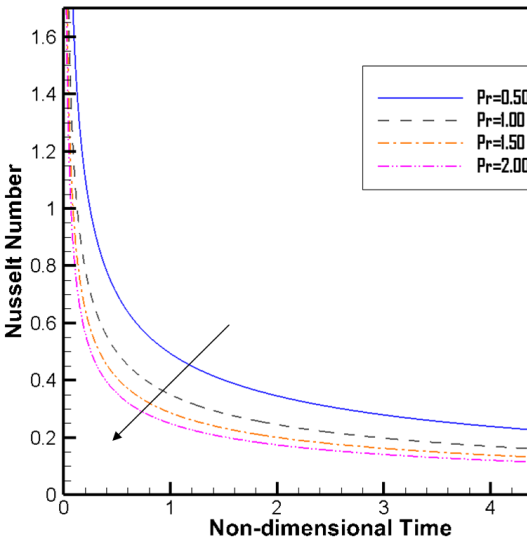

Figure 20: The impact of P_r on N_u

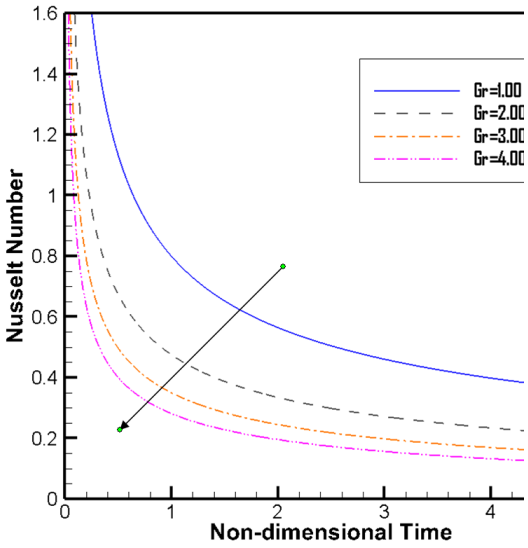

Figure 21: The impact of G_r on N_u

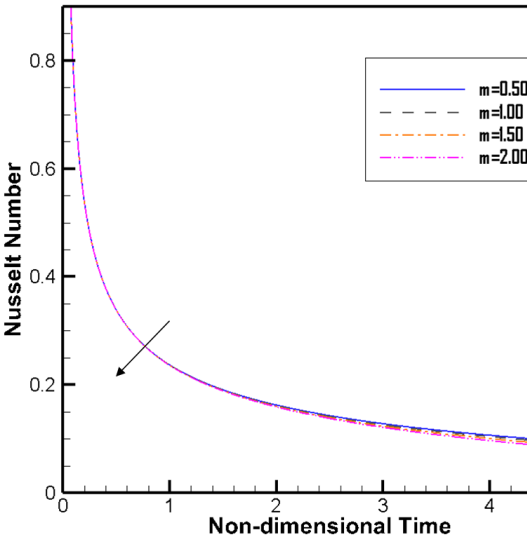

Figure 22: The impact of m on N_u

7. Conclusions

In this paper, the numerical solution of unsteady MHD MPF flow past a moving vertical plate with periodic field and Hall current effects is analyzed. The principal observations are given below:

- It is observed that the primary velocity profiles decrease for increasing data of M and P_r. Moreover increasing G_r and m caused the primary velocity profiles to increase.

- The behaviour of SVP decrease for M and P_r. Also increase for G_r and m.
- AVP increases qualitatively with the increasing values of M and P_r and decreases with increasing values of G_r and m.
- The skin friction distribution is falling for M and P_r and raising for G_r and m.
- Nu is an increasing function of M and decreases for P_r, G_r and m.

Acknowledgements. The author expresses sincere gratitude to the anonymous referee for their valuable comments, constructive feedback, and insightful suggestions, which have significantly improved the clarity, quality, and overall presentation of this paper.

Author's Contributions. All authors have contributed equally to the research and preparation of this work.

Conflict of Interest. The authors declared no potential conflicts of interest with respect to the research.

REFERENCES

1. A.C. Eringen, Theory of micropolar fluids, *Journal of Mathematics and Mechanics*, 16 (1966) 1–18.
2. T.Y. Na and I. Pop, Boundary-layer flow of micropolar fluid due to a stretching wall, *Archives of Applied Mechanics*, 67(4) (1997) 229–236.
3. A. Desseaux and N.A. Kelson, Flow of a micropolar fluid bounded by a stretching sheet, *ANZIAM Journal*, 42(E) (2000) C536–C560.
4. F.M. Hady, On the solution of heat transfer to micropolar fluid from a non-isothermal stretching sheet with injection, *International Journal of Numerical Methods for Heat and Fluid Flow*, 6(6) (1996) 99–104.
5. E.M. Abo-Eldahab and A.F. Ghonaim, Convective heat transfer in an electrically conducting micropolar fluid at a stretching surface with uniform free stream, *Applied Mathematics and Computation*, 137 (2003) 323–336.
6. A.A. Mohammadein and R. Gorla, Heat transfer in a micropolar fluid over a stretching sheet with viscous dissipation and internal heat generation, *International Journal of Numerical Methods for Heat and Fluid Flow*, 11(1) (2001) 50–58.
7. A.A. Mohammadein and R.S.R. Gorla, Effects of transverse magnetic field on mixed convection in a micropolar fluid on a horizontal plate with vectored mass transfer, *Acta Mechanica*, 118 (1996) 1–12.
8. G.W. Sutton and A. Sherman, *Engineering Magnetohydrodynamics*, McGraw-Hill, New York (1965).
9. G. Mandal and K.K. Mandal, Effect of Hall current on MHD Couette flow between thick arbitrarily conducting plates in a rotating system, *Journal of the Physical Society of Japan*, 52 (1983) 470–477.
10. S.K. Ghosh, Effects of Hall current on MHD Couette flow in a rotating system with arbitrary magnetic field, *Czech Journal of Physics*, 52 (2002) 51–63.
11. M.R. Raghavachar and V.S. Gothandaraman, Hydromagnetic convection in a rotating fluid layer in the presence of Hall current, *Geophysical and Astrophysical Fluid Dynamics*, 45(3) (1989) 199–211.

12. S.K. Ghosh and P.K. Bhattacharjee, Hall effects on steady hydromagnetic flow in a rotating channel in the presence of an inclined magnetic field, *Czech Journal of Physics*, 50(6) (2000) 759–767.
13. T. Hayat, S. Nadeem, S. Asghar and A.M. Siddiqui, Effects of Hall current on unsteady flow of a second grade fluid in a rotating system, *Chemical Engineering Communications*, 192 (2005) 1272–1284.
14. S.K. Ghosh, O.A. Beg and M. Narahari, Hall effects on MHD flow in a rotating system with heat transfer characteristics, *Meccanica* (2009), DOI: 10.1007/s11012-009-9210-6.
15. S.M. Arifuzzaman, B.M.J. Rana, R. Ahmed and S.F. Ahmmed, Cross diffusion and MHD effects on a high order chemically reactive micropolar fluid of naturally convective heat and mass transfer past an infinite vertical porous medium with a constant heat sink, *AIP Conference Proceedings* (2017), DOI: 10.1063/1.4984635.
16. S. Ahmad, H. Takana, H.G. Castellanos, K. Muzammil, S. Islam, Y. Aryanfar, M.A. Khan, M. Mursaleen and A.S. Hendy, Uncovering the mystery of the vortex dynamics in a micropolar fluid with multiple magnetic field strips: A novel case study, *Case Studies in Thermal Engineering*, 53 (2024) 103716.
17. M.V. Krishna, N.A. Ahamad and A.F. Aljohani, Thermal radiation, chemical reaction, Hall and ion slip effects on MHD oscillatory rotating flow of micropolar liquid, *Alexandria Engineering Journal*, 60 (2021) 3467–3484.
18. L. Kumar, A. Singh, V.K. Joshi and K. Sharma, MHD micropolar fluid flow with Hall current over a permeable stretching sheet under the impact of Dufour–Soret and chemical reaction, *International Journal of Thermofluids*, 26 (2025) 101042.
19. P. Jalili, H. Narimisa, B. Jalili, A. Shateri and D.D. Ganji, A novel analytical approach to micropolar nanofluid thermal analysis in the presence of thermophoresis, Brownian motion and Hall current, *Soft Computing*, 27 (2023) 677–689.
20. M. Mishra, J.P. Panda and S.S. Sahoo, An analytical investigation of MHD natural convective flow of a polar fluid in two vertical concentric cylinders with Hall current and heat source, *International Journal of Applied and Computational Mathematics*, 10 (2024) 75.